Photophysics of Metalloazurins†

John E. Hansen,‡ James W. Longworth,§ and Graham R. Fleming*,‡

Department of Chemistry and James Frank Institute, The University of Chicago, Chicago, Illinois 60637, and Department of Physics, Illinois Institute of Technology, Chicago, Illinois 60616

Received August 30, 1989; Revised Manuscript Received April 20, 1990

ABSTRACT: The fluorescence lifetimes of Cu(II), Cu(I), Ag(I), Hg(II), Co(II), and Ni(II) azurin Pae from *Pseudomonas aeruginosa* and Cu(II), Cu(I), and Hg(II) azurin Afe from *Alcaligenes faecalis* were measured at 295 K by time-correlated single-photon counting. In addition, fluorescence lifetimes of Cu(II) azurin Pae were measured between 30 and 160 K and showed little change in value. Ultraviolet absorption difference spectra between metalloazurin Pae and apoazurin Pae were measured, as were the fluorescence spectra of metalloazurins. These spectra were used to determine the spectral overlap integral required for dipole–dipole resonance calculations. All metalloazurins exhibit a reduced fluorescence lifetime compared to their respective apoazurins. Forster electronic energy transfer rates were calculated for both metalloazurin Pae and metalloazurin Afe derivatives; both enzymes contain a single tryptophyl residue which is located in a different position in the two azurins. These azurins have markedly different fluorescence spectra, and electronic energy transfers occur from these two tryptophyl sites with different distances and orientations and spectral overlap integral values. Intramolecular distances and orientations were derived from an X-ray crystallographic structure and a molecular dynamic simulation of the homologous azurin Ade from *Alcaligenes denitrificans*, which contains both tryptophyl sites. Assignments were made of metal–ligand-field electronic transitions and of transition dipole moments and directions for tryptophyl residues, which accounted for the observed fluorescence quenching of Hg(II), Co(II), and Ni(II) azurin Pae and Cu(II) and Hg(II) azurin Afe. The fluorescence of azurin Pae is assigned as a ^1L_b electronic transition, while that of azurin Afe is ^1L_a. The marked fluorescence quenching of Cu(II) azurin Pae and Cu(I) azurin Pae and Afe is less well reproduced by our calculations, and long-range oxidative and reductive electron transfer, respectively, are proposed as additional quenching mechanisms. This study illustrates the application of Forster electronic energy transfer calculations to intramolecular transfers in structurally well characterized molecular systems and demonstrates its ability to predict observed fluorescence quenching rates when the necessary extensive structural, electronic transition assignment, and spectroscopic data are available. The agreement between Forster calculations and quenching rates derived from fluorescence lifetime measurements suggests there are limited changes in conformation between crystal structure and solution structures, with the exception of the tryptophyl residue of azurin Afe, where a conformation derived from a molecular simulation in water was necessary rather than that found in the crystal structure.

Azurin is a blue copper(II) protein found in denitrifying soil bacteria and is believed to be involved in electron transport to a terminal oxidase (Henry & Bessiere, 1984; Ryden, 1984; Ambler & Tobari, 1989). The Cu(II) ion is surrounded by four ligands in a distorted trigonal-planar pyramid arrangement (Baker, 1988)—see Figure 1. The three closest ligands are two histidines and a cysteine, almost equidistant from the Cu(II) ion, forming a trigonal structure. The fourth ligand is a methionine with a long bond length of 3.1 Å (Norris et al., 1986; Baker, 1988). When excited with ultraviolet light, apoazurins exhibit large fluorescence quantum yields, which have been attributed to fluorescence from their tryptophan residues. Azurin from *Alcaligenes denitrificans* (azurin Ade) contains a buried tryptophan at position 48 and an exposed tryptophan at position 118 (Ambler, 1973; Baker, 1988). Azurins from *Pseudomonas aeruginosa* (azurin Pae) and *Pseudomonas fluorescens* (azurin Pfl) contain a single tryptophan at the buried position 48 (Ambler, 1973; Ambler & Brown, 1967; Adman & Jensen, 1981), while azurin from *Alcaligenes faecalis* (azurin Afe) also contains a single tryptophan at the exposed position 118 (Ambler, 1973).

The tryptophan fluorescence in a native azurin is extensively quenched compared to that of its apoprotein (Finazzi-Agro et al., 1973; Szabo et al., 1983; Petrich et al., 1987; Hutnik & Szabo, 1989a). When Cu(II) is replaced with Cu(I), Ag(I), Hg(II), Co(II), or Ni(II), different amounts of fluorescence quenching are observed (Finazzi-Agro et al., 1973; McMillin et al., 1974; Tennent & McMillin, 1979; Grinvald et al., 1975; Hutnik & Szabo, 1989b). Fluorescence is not quenched when Cu(II) is replaced with either Cd(II) or Zn(II) (Engeseth & McMillin, 1986). The quenching of tryptophan fluorescence could result from several effects, perhaps in combination in some cases. In previous work (Petrich et al., 1987) we proposed that the fluorescence quenching of Cu(II) azurins occurs via an electron transfer. Long-range electronic energy transfer must also be considered, since in some metalloazurins there is significant absorbance in the region of tryptophan fluorescence. An additional quenching mechanism is an enhanced intersystem crossing as a result of the heavy-atom effect (Finazzi-Agro et al., 1973). The latter process seems unlikely in most systems because luminescence spectra, measured at 77 K, show that the fluorescence to phosphorescence ratio is the same for apoazurin Pfl and Cu(II), Ag(I), and Hg(II)-substituted azurin Pfl (Finazzi-Agro et al., 1973). In addition, heavy-atom quenching is not consistent with structural studies that place the tryptophan 11 Å away from the metal atom. Nevertheless, comparison of luminescence spectra measured

† This work was supported by NSF.

* Address correspondence to this author.

‡ The University of Chicago.

§ Illinois Institute of Technology.

0006-2960/90/0429-7329$02.50/0

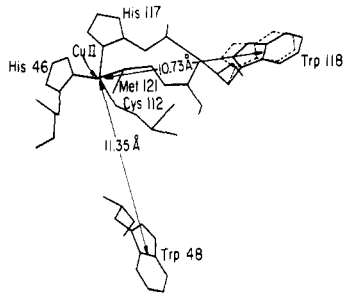

FIGURE 1: Position of tryptophans W48 and W118 with respect to the Cu(II) center determined from the crystal structure for native azurin Ade. Dotted lines show one position from a range of orientations predicted for indole from molecular dynamics simulations when W118 is exposed to solvent ($\chi_1 = 50°$, $\chi_2 = -75°$).

at 77 K from Cu(I) and native azurin Pfl shows a substantial decrease in the fluorescence to phosphorescence ratio, indicating an increased triplet formation in the Cu(I) derivative of azurin Pfl (Ugurbil et al., 1977). In this case the presence of the distant metal influences the intersystem crossing rate.

Our initial, naive, aim in this work was to explore the dependence of a putative electron-transfer rate on the free energy change in different metal derivatives of azurins from two bacterial species, *P. aeruginosa* and *A. faecalis*. We measured time-resolved fluorescence decays of azurin Pae and Afe substituted with a variety of metal cations. These measured fluorescence decay rates are compared to quenching rates predicted from either Marcus theory (Marcus & Sutin, 1985) for long-range electron transfer or Forster theory (Forster, 1965) for dipole–dipole electronic energy transfer. To properly calculate the electronic energy transfer rates, spectroscopic assignments for the electronic transitions involving a charge transfer between metal and ligands are required. In addition, the spectral overlap between absorption and fluorescence is required; therefore, we measured the absorption difference spectra between the metalloazurins and apoazurin Pae and the fluorescence spectra of the respective metalloazurins. Comparison of calculated and experimental rates suggests that the relative importance of electron transfer or energy transfer in the fluorescence quenching depends strongly on the specific metal and azurin studied. Thus, metalloazurins do not provide a simple series to study the free energy dependence of long-range electron transfer. This study does, however, provide additional insight into the spectroscopic assignments of the charge-transfer transitions between metals and their ligands and a detailed application of Forster theory of electronic energy transfer to series of structurally and spectroscopically defined molecules, where distances and orientations are known.

Materials and Methods

Native azurin Pae were purified from a low pathogenic strain of *P. aeruginosa* (ATCC 19429),[1] and Afe was purified from the type strain of *A. faecalis* (ATCC 8750), and both were provided to us by Professor R. Timkovich, Department of Chemistry, University of Alabama. The chemicals used were reagent grade; anhydrous $Co(II)Cl_2$, $Ni(II)Cl_2 \cdot 6H_2O$, and silver acetate were obtained from Aldrich. $Hg(II)Cl_2$ and $Zn(II)Cl_2$ were obtained from Fisher, and $Cu(II)Cl_2 \cdot 6H_2O$ was from Baker. The water used was house distilled and deionized and exhibited negligible fluorescence background.

Fluorescence lifetimes were measured in a time-correlated single-photon counting apparatus, which is described elsewhere (Chang et al., 1986). Fluorescence was collected in a J-Y H10 (Instruments SA) monochromator placed against the end window of a Hamamatsu R1645U microchannel plate. Fluorescence decays were collected with 10000 counts in the peak channel and a time scale of 20.5 ps/channel. The instrument response function for the fluorescence decays had a full width at half-maximum of 90 ps. Fluorescence decays were fitted to a sum of exponentials, and acceptable fits to the decays had a χ^2 between 1.00 and 1.20.

The difference absorption spectra were measured on a Perkin-Elmer 559A UV/vis spectrophotometer. Steady-state fluorescence spectroscopy was carried out with a Perkin-Elmer MPF-66 fluorescence spectrophotometer. Low-temperature fluorescence spectroscopy was carried out on a Perkin-Elmer MPF-4 fluorescence spectrometer. An Air Products closed-cycle cryogenic refrigerator with an HC-2 compressor, a DE202 expander, and a Series 5500 microprocessor-based temperature controller was used for low-temperature time-resolved and steady-state fluorescence spectroscopy.

Native azurin Afe was purified according to a procedure described by Petrich et al. (1987). Native azurin Pae was purified following a similar procedure, though this protein elutes from an ion exchange column between pH 4.3 and pH 4.5. The purity of the azurins was determined from the ratio of their absorbance at 625 nm to that at 280 nm. Purified native azurins Afe and Pae had A_{625}/A_{280} ratios of 0.54–0.55 and 0.55–0.58, respectively. Ascorbate was used to reduce native Cu(II) azurin to form the Cu(I) derivative, and the Cu(I) was removed by complexation with thiourea to form the apoprotein, (Blaszak et al., 1983).

Metalloazurin samples used in time-correlated single-photon counting were prepared in dialysis of apoazurin against a 50 μM concentration of the metal cation in a 0.1 M sodium acetate buffer at pH 7.5 for 12 h at room temperature. The samples were then dialyzed three times against 0.1 M sodium acetate at pH 7.5 for 6 h. Final samples had a volume of 4 mL with an absorption at 280 nm of ca. 0.2.

Metalloazurin Pae samples used for absorption difference and fluorescence spectroscopy were made to the same concentration as the sample of apoazurin Pae. The same volumetric pipet was used to take three aliquots of 2.00 mL from a solution of native azurin ($A_{625}/A_{280} = 0.58$) in 0.1 M sodium acetate at pH 5.0 with an absorption at 280 nm of about 1.8. One aliquot of native azurin was reduced to the Cu(I) derivative. Another aliquot was used to prepare apoazurin. All three aliquots were then dialyzed against 0.1 M sodium acetate at pH 5.0, with three dialyzate changes over a period of 12 h. They were then brought to a volume of 5.00 mL with the same volumetric flask. To confirm the reproducibility of this procedure, two samples of apoazurin were treated separately and the difference spectra determined and found to be within 1% of the base line determined previous to dialysis treatment. Absorption difference spectra were taken between native Cu(II) and apoazurin, between Cu(I) azurin and apoazurin, and between Cu(I) azurin and native Cu(II) azurin.

To prepare the other samples [Ag(I), Hg(II), reconstituted Cu(II), and apo derivatives of azurin Pae], four aliquots of 2 mL each were taken from a solution of apoazurin Pae in 0.1 M sodium acetate at pH 7.5, with an absorption of about 1.8. To three of the four aliquots was added 2–3 equiv of the particular metal cation directly. Samples were then dialyzed against 0.1 M sodium acetate at pH 7.5 for 6 h at room temperature. All four aliquots were then dialyzed against 0.1 M sodium acetate at a pH of 5.0 with three dialyzate changes over 12 h. Difference absorption spectra were taken between Ag(I) azurin and apoazurin, between Hg(II) azurin and

[1] In Petrich et al. (1987) the strain number was inadvertently misnumbered, and in that paper this strain number was utilized.

Table I: Fluorescence Lifetimes of Metalloazurins[a]

azurin	temp (K)	pH	A_1	τ_1	A_2	τ_2	A_3	τ_3	F	k_{MI} ($\times 10^{-9}$ s^{-1})	ref
Cu(II) Pae	297	5.0	0.97 ± 0.01	104 ± 4 ps	0.03 ± 0.01	4.23 ± 0.1 ns			0.44	9.41	Hansen et al., 1988
	158	7.5	0.93 ± 0.01	110 ± 6 ps	0.03 ± 0.01	1.87 ± 0.1 ns	0.04 ± 0.01	6.72 ± 0.1 ns		8.97	
	98	7.5	0.94 ± 0.01	107 ± 6 ps	0.02 ± 0.01	1.60 ± 0.1 ns	0.05 ± 0.01	6.04 ± 0.1 ns		9.14	
	51	7.5	0.94 ± 0.01	115 ± 6 ps	0.02 ± 0.01	980 ± 100 ps	0.05 ± 0.01	5.60 ± 0.1 ns		8.49	
	34	7.5	0.93 ± 0.01	113 ± 6 ps	0.03 ± 0.01	550 ± 100 ps	0.04 ± 0.01	5.18 ± 0.1 ns		8.65	
Cu(I) Pae	297	5.0	0.87 ± 0.01	68 ± 8 ps	0.07 ± 0.02	760 ± 60 ps	0.06 ± 0.02	3.95 ± 0.1 ns	0.15	15.2	Hansen et al., 1988
Ni(II) Pae	297	7.5	0.79 ± 0.01	104 ± 4 ps	0.21 ± 0.01	4.56 ± 0.1 ns			0.079	9.42	Hansen et al., 1988
Co(II) Pae	297	7.5	0.74 ± 0.04	85 ± 6 ps	0.26 ± 0.04	4.70 ± 0.1 ns			0.049	11.6	Hansen et al., 1988
Zn(II) Pae	297	7.5	1.0	4.34 ± 0.04 ns						0.0273	Hansen et al., 1988
Hg(II) Pae	297	7.5	0.95 ± 0.01	380 ± 5 ps	0.05 ± 0.01	3.2 ± 0.2 ns			0.71	2.43	Hansen et al., 1988
	297	5.0	0.97 ± 0.01	369 ± 5 ps	0.03 ± 0.01	3.3 ± 0.3 ns			0.82	2.51	
	297	4.0	0.98 ± 0.01	359 ± 5 ps	0.02 ± 0.01	3.3 ± 0.3 ns			0.87	2.59	
Ag(I) Pae	297	5.0	1.0	3.22 ± 0.02 ns						0.109	
apo Pae	297	5.0	1.0	4.94 ± 0.02 ns							Hansen et al., 1988
Cu(II) Afe	297	5.0	0.92 ± 0.01	212 ± 10 ps	0.08 ± 0.01	2.8 ± 0.1 ns			0.53	4.23	Petrich et al., 1987
Cu(I) Afe	297	5.0	0.65 ± 0.05	144 ± 10 ps	0.17 ± 0.03	755 ± 80 ps	0.18 ± 0.06	2.90 ± 0.2 ns	0.62	6.33	Hansen et al., 1988
Hg(II) Afe	297	7.5	0.70 ± 0.01	690 ± 20 ps	0.30 ± 0.01	2.21 ± 0.1 ns			0.58	0.839	Hansen et al., 1988
apo Afe	297	5.0	0.43 ± 0.01	1.06 ± 0.06 ns	0.57 ± 0.01	2.79 ± 0.3 ns					Petrich et al., 1987

[a] Samples were excited with 292-nm light, and fluorescence was collected at 330 and 340 nm for metal derivatives of azurin Pae and Afe, respectively. Fluorescence decays had an instrument response function of approximately 90 ps. The peak channel in the decays contained 10000 counts. Fluorescence decays were fitted to a sum of exponentials, and an adequate fit had a χ^2 between 1.00 and 1.20. The column labeled k_{MI} list the metal-induced nonradiative rates, which were calculated by subtraction of the inverse of the fluorescence lifetime of the apoprotein from the inverse of the lifetime of the fast component of the fluorescence decay of the metalloazurin. The fraction of total fluorescence from the short lifetime component is also listed.

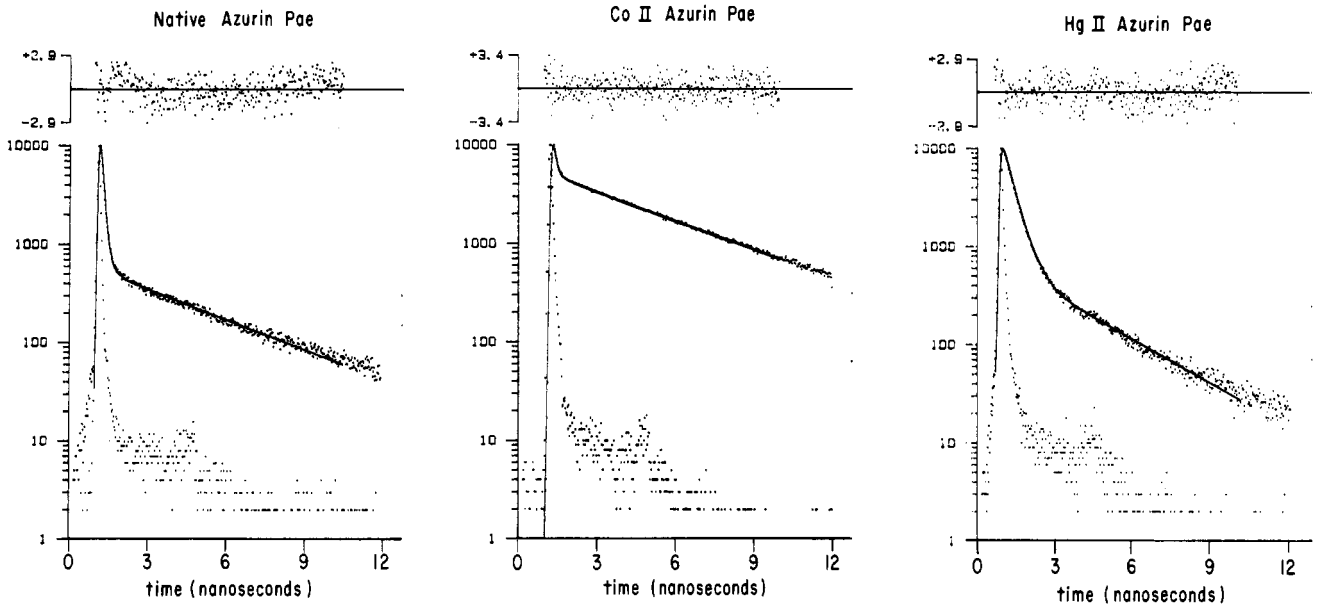

FIGURE 2: Fluorescence decays of native Cu(II), Co(II), and Hg(II) azurin Pae. Decays are fitted to a sum of two exponentials, and plots of the weighted residuals for the fits are shown. Instrument response function for the fits is approximatley 90 ps FWHM.

apoazurin, and between reconstituted Cu(II) azurin and apoazurin.

Samples of native azurin Pae for low-temperature studies were first lyophilized from a buffer of 0.05 M Na_2HPO_4 and 0.05 M NaCl at pH 7.5 and then dissolved in a solution of 50% ethylene glycol and 50% water. This solution had an absorbance at 280 nm of 1.0 in a 1-cm cell. The sample was then placed in a Supersil quartz tube with a 4-mm o.d. and a 2.4-mm i.d., which had been cleaned in nitric acid. The sample was rapidly cooled to a temperature of 77 K with liquid nitrogen and then quickly put under vacuum and cooled to 30 K. Fluorescence was collected from the front surface, about 30° to the incident beam. The temperature was then raised successively from 30 to 160 K, 20 K below the glass transition.

Results

(A) Fluorescence Decay Data. Table I presents the results of fits of the fluorescence decay data to sums of exponentials. The major short component in these fits is attributed to the quenching process, and the minor long (4.4 ns) component is attributed to an "apo-like" impurity that is unable to bind metal ligands (Petrich et al., 1987). In the low-temperature Cu(II) data there is an intermediate lifetime component that arises from an impurity in the ethylene glycol used in the solvent. Several points stand out in the data. First, the lifetime of the major short component in native azurin Pae (W48) is almost independent of temperature. Second, the short decay components in the Cu(I) and Co(II) Pae systems are significantly shorter than those of the native protein. In the case of Cu(I) a third low-amplitude decay component was required for satisfactory fits to the data. We do not know the origin or this component. Zn(II) produces little if any quenching of W48, whereas Hg(II) produces substantial quenching and Ag(I) produces modest quenching. Figure 2 compares the decay curves of Cu(II), Co(II), and Hg(II) azurin Pae. Note that, as pointed out in our earlier work (Petrich et al., 1987), the presence of a long lifetime component in the decays makes steady-state measurements unreliable estimates of the degree

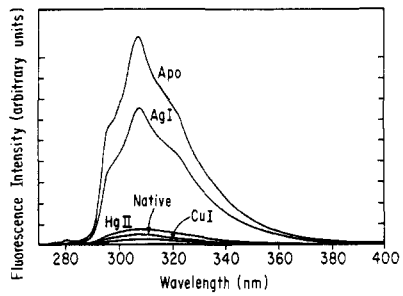

FIGURE 3: Emission spectra from several metal derivatives of azurin Pae are compared to that from an equal concentration of apoprotein. 280-nm light was used for excitation.

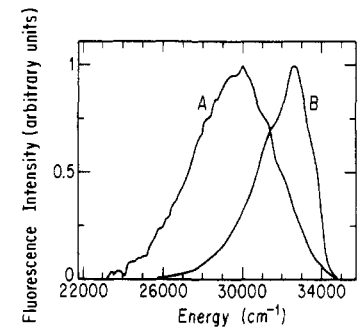

FIGURE 4: Fluorescence spectra of apoazurin Afe (A) and Pae (B) [redrawn from Figure 4 of Petrich et al. (1987)].

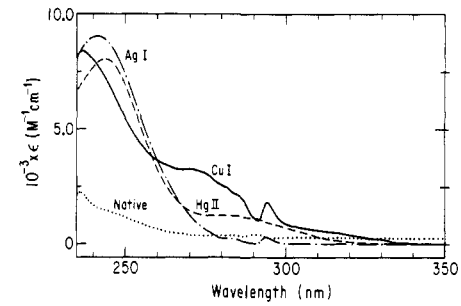

FIGURE 5: Absorption difference spectra of metal derivatives of azurin Pae using apoazurin Pae in 100 mM sodium acetate at pH 5 as a reference: native Cu(II) (···); Cu(I) (—); Hg(II) (– –); Ag(I) (–·–) azurin Pae.

of quenching. For example, Tennent and McMillin (1979) report that the fluorescence of Ni(II) azurin Pae is quenched 70% compared with that of the apoprotein, whereas the lifetime (using only the short component) decreases 52-fold. The steady-state fluorescence is dominated by the contribution from the long lifetime component. Despite the similarity in lifetime it seems unlikely that this long component is apoazurin Pae since studies of thermally induced denaturation of Ni(II) and Co(II) azurin Pae by differential scanning calorimetry (Engeseth & McMillin, 1986) reveal no evidence for its existence. However, of the metal derivatives of azurin Pae studied, only derivatives of Co(II) and Ni(II) exhibit two peaks in their calorimetric scans. Engeseth and McMillin suggest this is a result of weak binding of the metal cations.

Though more limited, the data for quenching of W118 in metalloazurins Afe show parallel trends to the Pae metalloazurins. Particularly striking is the similarity in the ratios of the short components for the two species: $\tau(\text{Afe})/\tau(\text{Pae}) = 2.0$ [Cu(II)], 2.25 [Cu(I)], and 1.84 [Hg(II)]. If the metal-induced nonradiative rates are used (Table I, calculated by subtraction of the inverse of the lifetime of the apoazurin from the inverse of the fast decay component), the ratios are 2.3:1, 2.4:1, and 2.5:1 for these three metals.

Recently, Hutnik and Szabo (1989a) reported measurements for the fluorescence decay rates of Cu(I) and Cu(II) azurin Pae. Their values for the time constant of the short decay component agree with the values we previously reported for Cu(I) azurin Pae (Hansen et al., 1988) and Cu(II) azurin Pae (Petrich et al., 1987; Hansen et al., 1988). However, they find it necessary to fit the fluorescence decay of native Cu(II) azurin to a sum of three exponentials, whereas we find a two-component fit sufficient. Of all the metalloazurins Pae we studied, only Cu(I) azurin Pae has a fluorescence decay for which we find it necessary to invoke a three-component fit (see Table I). It is interesting to compare the values we obtain for the short component in the fluorescence decays of Ni(II) and Co(II) azurin Pae to those of Ni(II) and Co(II) azurin Pfl obtained by Hutnik and Szabo (1989b). The short decay component of both Ni(II) azurin Pae and Ni(II) azurin Pfl have the same time constant, while the short decay component for Co(II) azurin Pfl has a time constant 50% longer than that for Co(II) azurin Pae. Of the four metal derivatives of azurin Pae and Pfl, only the Co(II) derivatives have differing short components in their fluorescence decays.

(B) Absorption and Emission Spectra. The fluorescence spectra of all the metal derivatives of each azurin were indistinguishable (see Figure 3). Figure 4 shows representative spectra for azurin Pae and azurin Afe. Note the substantial red shift in fluorescence for azurin Afe (W118) compared with that for azurin Pae (W48). Because of the large difference in lifetimes between the long and short decay components, a small amplitude for the long decay component is sufficient to contribute a substantial fraction of the steady-state spectrum to the long component. The fraction of the steady-state spectrum arising from the short component is listed in Table I. For Cu(II), Hg(II), and Ag(I) azurin Pae the steady-state fluorescence spectrum is dominated by the short component. Note that these metalloazurins have a fluorescence spectrum identical with that of the apoprotein (see Figure 2). We have assumed that this also applies to these metalloazurins where the steady-state spectrum has a substantial contribution from a long lifetime component [e.g., Co(II) azurin Pae].

To calculate rates for energy transfer from tryptophan to acceptors such as metal–ligand charge-transfer bands, accurate absorption spectra and spectral transition assignments are required. Absorption spectra of acceptors in the native, Cu(I), Hg(II), and Ag(I) azurins are not readily accessible, since they have weak absorptions that are buried under the comparatively strong absorption from tryptophan. Absorption spectra for these acceptors were obtained from an absorption difference spectrum between a metalloazurin Pae and apoazurin Pae. Difference spectra for several metalloazurins Pae are shown in Figure 5. There is similarity between these absorption difference spectra and those measured in analogous metalloplastocyanins (Tamilarasan & McMillin, 1985). The similarity is marked at the longer wavelength region, which is the relevant spectral region to this study. A notable feature is the appearance of a "typical" tryptophan difference band (Donovan, 1969) centered at 293 nm in the metalloazurin difference spectra, which is absent in the corresponding difference spectra of the metalloplastocyanins. We find a greater absorption at 242 nm for the Ag(I) azurin than for Ag(I) plastocyanin, and there is a 4-nm red shift of a corresponding high-energy absorption peak in Hg(II) plastocyanin compared with the Hg(II) azurin. A difference spectrum between Cu(II) azurin Pae and Cu(I) azurin Pae was also measured (Figure 6) and found to be identical, within experimental error, with the difference spectrum reported by Pecht et al. (1976). Pecht et al. reduced Cu(II) azurin Pae with a hyrogen electrode,

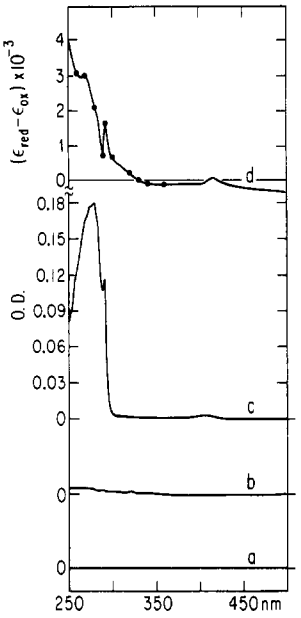

FIGURE 6: Absorption difference spectrum between Cu(II) azurin Pae and Cu(I) azurin Pae: (a) buffer – buffer, 100 mM sodium acetate, pH 5; (b) Cu(II) azurin Pae – Cu(I) azurin Pae, pH 5. (c) Absorption spectrum of Cu(II) azurin Pae, pH 5. (d) Difference spectrum of Cu(II) azurin Pae – Cu(I) azurin Pae; solid points taken from a difference spectrum of Pecht et al. (1977).

which was presumed not to alter the protein concentration, while the difference spectrum shown in Figure 6 was produced by comparing two separately prepared samples. These difference spectra involve two metalloazurins with very different stabilities; Cu(I) azurin binds copper less avidly than Cu(II) azurin (Blaszak et al., 1983). Nevertheless, the similarity shown in Figure 6 suggests that a difference in metalloazurin stability does not affect difference spectra measured on samples prepared by separate procedures. A feature to note is that the tryptophan difference in the Cu(I) azurin difference spectrum is much larger than that of other metalloazurin difference spectra; moreover, there is no observable tryptophan difference in the Hg(II) azurin difference spectrum (Figure 5). It appears that the environment of the tryptophan is perturbed more in Cu(I) azurin Pae than it is in the other metalloazurins and imperceptibily altered in Hg(II) azurin Pae, by comparison with the apoazurin Pae. Tryptophan absorption of Cu(I) and Ag(I) azurin Pae is shifted to lower energies compared to that of apoazurin, while that for native Cu(II) azurin is shifted to higher energies. The spectral shift in tryptophyl absorption may be related to a change in the Coulombic interaction of the tryptophan with the protein surface charges. A spectral shift of the tryptophan absorption caused by conformational changes or from changes in solvent environmental seems very unlikely. The tryptophan residue of azurin Pae is deeply buried in the protein and is in a hydrophobic region of the protein. More significant is that the fluorescence spectrum is independent of metallation and has an unusually small Stokes shift. Theoretical studies have indicated that a change in charge distribution at the protein surface occurs when native Cu(II) azurin is reduced (Bashford et al., 1988). We find that divalent metal cations produce a blue shift of the tryptophan absorption, whereas monovalent metal cations produce a red shift with reference to the tryptophan absorption in apoazurin.

In comparison with that of native Cu(II) azurin Pae, the difference spectrum of reconstituted Cu(II) azurin Pae has about 25% greater absorption between 240 and 380 nm (Figure 7) and there is a corresponding 4–6% increase in the amplitude

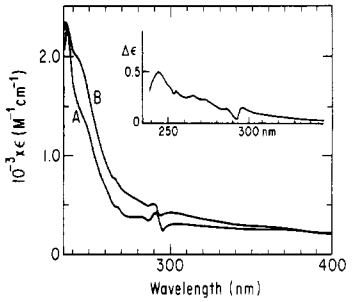

FIGURE 7: Absorption difference spectra of (A) native Cu(II) and (B) reconstituted Cu(II) azurin Pae using apoazurin in 100 mM sodium acetate at pH 5 as reference. Inset shows an absorption difference spectrum between reconstituted Cu(II) azurin Pae and native Cu(II) azurin Pae.

of the long lifetime component to the fluorescence decay of reconstituted azurin Pae. Note that in the difference spectrum between reconstituted Cu(II) azurin Pae and native Cu(II) azurin Pae (Figure 6) the tryptophan difference at 290 nm shows a red shift compared to a blue shift seen in the difference spectrum between native Cu(II) azurin Pae and apoazurin Pae. Also, the ratio of absorption at 625 nm to that at 280 nm for reconstituted azurin Pae is 0.53 compared to 0.58 for native azurin Pae. These absorptions are similar to those reported by Blaszak et al. (1983) and suggest that the long decay component found in all metalloazurins may arise in a protein that has suffered specific chemical modification of the binding site and cannot bind metal cations.

The limited quantities of protein available to us did not allow us to measure analogous difference spectra for the azurin Afe derivatives. However, since there is such a similarity between the difference spectra of metalloazurins Pae and the analogous metalloplastocyanins, for wavelengths longer than 260 nm, we expect very similar difference spectra for the analogous metalloazurins Afe. Accordingly, the Pae difference spectra were used to calculate the overlap integrals for the metalloazurins Afe.

Discussion

(A) Binding of the Metals. Previous work provides strong evidence that the metal cations used in this study bind to the site where Cu(II) is bound in blue copper proteins (Finazzi-Agro et al., 1973; Tennent & McMillin, 1979; Engeseth & McMillin, 1984, 1986; Hauenstein & McMillin, 1981; Live et al., 1985; Tamilarasan & McMillin, 1986; Colman et al., 1978). X-ray studies have shown that when the Cu(II) cation is removed from poplar plastocyanin, the positions of the ligands are almost unaffected, except for a ring rotation of imidazole of His87 (Garrett et al., 1984). Further, when Cu(II) is replaced by Hg(II), the deviations in the positions of the ligands are remarkably small (Church et al., 1986). This suggests that the ligands of poplar plastocyanin are constrained by the protein structure. The ligands surrounding the Cu(II) cation in azurin Ade have positions very similar to those in poplar plastocyanin (Ainscough et al., 1987; Baker et al., 1988); thus, replacement of the Cu(II) cation of azurin by other metal cations should have minimal effects on their positions. In fact, as Baker (1988) points out in the crystal structure of native Cu(II) azurin Ade, constraints imposed by the protein upon the copper site make it the most rigid and well-ordered part of the structure.

Cu(II) azurin Ade is currently the only azurin for which a 1.8-Å high-resolution crystal structure exists (Norris et al., 1986; Baker, 1988). A 2.7 Å resolution crystal structure is known for Cu(II) azurin Pae (Adman & Jensen, 1981), and this structure shows a high degree of topological homology with

the azurin Ade structure (Norris et al., 1983), as does the 3.0-Å crystal structure for azurin Pde (*P. denitrificans*) (Korszum, 1987). There is, also, a high degree of sequence homology among azurins: with 64% sequence homology between azurin Pae and azurin Afe, 63% homology between azurin Pae and azurin Ade, 67% homology between azurin Afe and azurin Ade, and 86% homology between azurin Pae and azurin Pde (Ambler, 1973). It is therefore expected that a high degree of topological homology exists among all azurins (Adman & Jensen, 1981; Korszum, 1987; Baker, 1988), a feature observed in several other families of proteins (Richardson, 1981). Because of marked sequence and topological homologies, we have used the 1.8 Å resolution crystal structure of native Cu(II) azurin Ade (Baker, 1988) to identify the orientation and distance between the tryptophan residue, W48, and the metal center in azurin Pae and the orientation and distance between the tryptophan residue, W118, and the metal center in azurin Afe. However, W118 is exposed at the periphery of the hydrophobic patch at the northern end of azurin. Its position was shown to be affected by solvent in molecular dynamics simulations of Chen et al. (1988). We used this simulation to find a range of orientations for W118 that could explain its fluorescence quenching. W48 is buried in the protein, and its available orientations are limited. This is borne out in the molecular dynamics simulations and in comparison of the two distinguishable molecules in the X-ray crystallographic study of azurin Ade (Baker, 1988; see Figure 5). The average orientation of W48 in the molecular dynamics simulations is the same as that found in the crystal structure. We used molecule A of the two distinguishable molecules of azurin Ade that make up the asymmetric unit cell to obtain orientations and distances necessary for calculating the rates of electronic energy transfer listed in Table IV. Calculations for rates of energy transfer for tryptophan 48 based on orientations and distances obtained from molecule B were compared to those from molecule A and found to be about 20% less. These differences in rates are within calculated error. As mentioned above, we have calculated rates of energy transfer for the tryptophans in the metal derivatives of azurins Pae and Afe on the basis of orientations and distances from the crystal structure of azurin Ade. Small differences in position of the metal ligands and analogous tryptophans among the azurins can introduce significant changes in our calculations. Also, using a molecular model derived from a crystal structure to represent these proteins in solution may also introduce further uncertainties and changes in position not already mentioned. These cumulative effects could result in calculated rates that differ by up to 50%.

(*B*) *Fluorescence Quenching of Tryptophan.* To discuss the metal-induced nonradiative rates of Table I, we consider three possible mechanisms for fluorescence quenching: electronic energy transfer, reductive fluorescence quenching, and oxidative fluorescence quenching.

(*1*) *Electronic Energy Transfer.* The rate of energy transfer between a donor and acceptor that are electronically coupled through a dipole–dipole interaction can be calculated from Forster theory (Forster, 1948, 1959). The rate is given by

$$k = \frac{9(\ln 10)\Phi_D\kappa^2}{128\pi^5\eta^4 N\tau_D R^6}\int_0^\infty \frac{F(\nu)\epsilon(\nu)\,d\nu}{\nu^4}$$

where Φ_D is the quantum yield of the donor, η is the refractive index of the medium, N is Avogardro's constant, τ_D is the excited donor lifetime in absence of acceptors, R is the distance between donor and acceptor $\epsilon(\nu)$ is the decadic molar extinction coefficient at wavenumber ν, $F(\nu)$ is the donor fluorescence intensity at ν (normalized to unit area on a wavenumber scale), and κ^2 describes the orientation between donor and acceptor. The expression for the orientation factor κ^2 is given by

$$\kappa^2 = (\cos\theta - 3\cos\theta_A\cos\theta_D)^2$$

where θ is the angle between the transition dipole moments, θ_D is the angle between the emission dipole moment and the line connecting the dipole moments, and θ_A is the angle between the absorption dipole moment and the line connecting the dipole moments. The angles are determined from the crystal structure of azurin Ade. The two lowest singlet excited states of indole derivatives are close in energy and described as ^1L_a and ^1L_b, their relative energies being determined by environment (Strickland, 1974; Lami & Glasser, 1986). The absorption and fluorescence of the ^1L_b state is insensitive to changes in the solvent polarity, while the ^1L_a state is strongly red shifted when the indole is in aqueous surroundings (Lami & Glasser, 1986). Szabo et al. (1983) noted the similarity between the fluorescence of 3-methylindole in a hydrocarbon and the fluorescence of W48 tryptophan in azurin. The study of Lami and Glasser (1986) suggests that the fluorescence from the W48 tryptophan originates from a ^1L_b state, while the fluorescence from the W118 tryptophan originates from a ^1L_a state. Further support for these assignments is provided by the electronic energy transfer calculations from W48 to W118 in azurin Ade (Chen et al., 1988), which are only consistent with experiment with the above assignments and not with a ^1L_a W48 fluorescence. In addition, the two-state model developed for the fluorescence of tryptophan by Ruggiero et al. (1990) defined a ^1L_b fluorescence spectrum consistent with the W48 fluorescence of azurins. The directions we use for the emission transition dipole moments for the ^1L_a and ^1L_b states in W48 and W118 are based on experimental and theoretical studies of tryptophan and other indole derivatives (Yamamoto & Tanaka, 1972; Negus & Hochstrasser, 1984; Negus, 1985; Rehms & Callis, 1987; Philips & Levy, 1986). We take the transition dipole moment for ^1L_a (W118) to lie between −20° and −24° to the long axis of indole ring and the transition moment for ^1L_b (W48) to lie between +66° and +70° to the long axis. In Tables II and III we show how sensitive the orientation factor is to the angle of the ^1L_b and ^1L_a transition moment to the long axis of the indole ring of tryptophans 48 and 118, respectively.

For azurins Pae and Afe the relevant overlap regions are 285–390 nm and 285–435 nm, respectively. In this region only metal–ligand charge-transfer transitions are expected to carry significant oscillator strength. There may be several different transitions contributing to the overlap region [see, for example, Table 8.2 of Lever (1984)]. Both sulfur and imidazole ligand-to-metal charge-transfer (LMCT) transitions may lie in the 300–400-nm wavelength range (Lever, 1984). In addition, because of the change in reduction potentials between the various metals, there are substantial shifts of individual transitions for different metal-substituted proteins. For example, the characteristic red absorption band (625 nm) of Cu(II) azurin is assigned to charge transfer from the cysteine sulfur to the Cu(II) cation. In Co(II) azurin this band is shifted to 385 nm in accord with the greater difficulty of reducing Co(II). In view of the uncertainties in assignment and the possibilities of different transitions dominating the overlap in the different derivatives, or between azurins Pae and Afe, for example, we have calculated energy transfer rates for all possible transitions.

The absorption transition dipole moments of the metal–ligand transitions involved in fluorescence quenching are assumed to be along one of the ligand to metal bonds. We also

Table II: Orientation between the Emission Dipole Moment of Tryptophan 48 and the Metal to Ligand Bonds[a]

bond	$\Phi = 50°$	$\Phi = 60°$	$\Phi = 65°$	$\Phi = 70°$	$\Phi = 80°$	$R \pm 0.12$ Å
Cu–His46	0.1 ± 0.2	0.11 ± 0.19	0.11 ± 0.17	0.11 ± 0.17	0.10 ± 0.15	11.56
Cu–His117	3.27 ± 0.12	2.85 ± 0.14	2.54 ± 0.15	2.31 ± 0.16	1.70 ± 0.17	12.29
Cu–Cys112	1.35 ± 0.16	1.39 ± 0.16	1.36 ± 0.16	1.33 ± 0.16	1.20 ± 0.16	10.60
Cu–P_y	1.64 ± 0.14	1.51 ± 0.15	1.39 ± 0.15	1.29 ± 0.15	1.02 ± 0.16	10.60
Cu–Met121	0.15 ± 0.2	0.29 ± 0.17	0.40 ± 0.16	0.47 ± 0.15	0.64 ± 0.12	11.21

[a] $\kappa^2 = (\cos\theta - 3\cos\theta_A \cos\theta_D)$, described in the text. Φ is the angle between the transition emission dipole moment and the long axis of the indole ring in W48. R is the distance between the centers of the emission transition dipole moment in W48 and the bond between ligand and metal. M–His46, M–His117, M–Cys112, and M–Met121 refer to an absorption transition dipole moment along the respective metal to ligand bond. M–P_y refers to the absorption transition dipole moment along the line connecting the metal cation to the P_y orbital of sulfur in Cys112.

Table III: Orientation between the Emission Dipole Moment of Tryptophan 118 and the Metal to Ligand Bonds[a]

bond	$\Phi = -20°$	$\Phi = -24°$	$\Phi = -30°$	$R \pm 0.12$ Å
Cu–His46	2.37 ± 0.15	2.12 ± 0.16	1.74 ± 0.17	11.44
Cu–His117	0.39 ± 0.18	0.28 ± 0.17	0.15 ± 0.16	10.14
Cu–Cys112	0.24 ± 0.16	0.19 ± 0.16	0.12 ± 0.16	10.03
Cu–P_y	0.16 ± 0.16	0.11 ± 0.16	0.04 ± 0.15	10.03
Cu–Met121	0.32 ± 0.15	0.36 ± 0.14	0.40 ± 0.15	10.40

[a] Look at the footnotes to Table II. The orientation used for the indole of W118 is one from a range of orientations predicted by molecular dynamics simulations. The dihedral angles χ_1 and χ_2 for the orientation of indole used in this table are 50° and −75°, respectively.

considered the direction of the dipole moment along the line connecting the P_y orbital of the thiolate sulfur to the metal cation, determined from spin-restricted self-consistent-field Xα-scattered wave (SCF-Xα-SW) calculations (Penfield et al., 1985; Solomon et al., 1985). Directions for the ligand to metal bonds were determined from the 1.8-Å crystal structure of azurin Ade (Baker, 1988). The line connecting the P_y orbital of the thiolate sulfur to the Cu(II) cation lies in a plane containing the γ-sulfur and β-carbon of Cys112 and the Cu(II) cation, about 20° to the line connecting the centers of the thiolate sulfur and the Cu(II) cation that points toward the β-carbon. Orientation factors, κ^2, were calculated from orientations between the fluorescence-transition dipole moment of tryptophan W48 of azurin Pae with respect to the five possible orientations of an absorption-transition dipole moment for a metal center transition (Table II). Orientation factors were also calculated for several angles centered around an angle of +66° for the fluorescence-transition dipole moment of W48 with respect to the long axis of the indole ring. As can be seen, κ^2 is not very sensitive to the angle between the ^1L_b transition moment and the long axis of the indole ring of W48. When calculating κ^2 values for orientations between the ^1L_a transition moment of W118 and the five possible absorption dipole moments (see Table III), we considered orientations of the indole ring provided by dynamic simulations of azurin Ade. Using crystal structure coordinates for the indole of W118, we were not able to explain the observed rate of quenching in any of the metal derivatives of azurin Afe from energy transfer calculations. This orientation of the indole of W118 appears to arise from the way the crystal packs. W118 is located on a hydrophobic patch where two azurin molecules contact in the asymmetric unit of the crystal. Consequently, this particular orientation for the indole may not be representative of W118 exposed to solution. However, rotation of the indole about the χ_1 and χ_2 bonds as indicated from dynamic simulations of azurin Ade in the presence of solvent [see Figure 9 of Chen et al., (1988)] does provide a range of orientations that can explain the fluorescence quenching in Hg(II) and native azurin Afe as electronic energy transfer. These orientations for the indole have a χ_1 dihedral angle between −70° and −80° (a mean value of about −75° is observed for the χ_1 dihedral angle during the simulation) and a χ_2 dihedral angle between +50° and +60° (a mean value of about +63° for the χ_2 dihedral angle is observed during the last 15 ps of the simulation).

Overlap integrals were calculated from the measured absorption spectrum for the acceptor and the fluorescence spectrum of the donor, as described above, and the values are listed in Table IV. For Cu(I), Hg(II), Ag(I), and native azurin Pae and Afe the overlap integrals were calculated with their respective difference spectra.

Calculations of overlap integrals for Ni(II) and Co(II) azurin Pae use the absorption spectra of Lum and Gray (1974) and McMillin et al. (1974), respectively. We assume here that the majority of the overlap occurs for wavelengths greater than 300 nm. We did not consider any absorption that may exist under the tryptophan absorption when calculating these overlap integrals. Thus, the overlap integrals for Ni(II) and Co(II)

Table IV: Calculated Rates of Electronic Energy Transfer

azurin	J_{AD} ($\times 10^{13}$ mol^{-1} cm^{-1})	rates ($\times 10^{-9}$ s^{-1}) M–His	M–Cys	M–P_y	M–Met	obsd rate ($\times 10^{-9}$ s^{-1})
Cu(II) Pae	2.66 ± 0.3	2.17 ± 0.5	5.3 ± 1	5.4 ± 1	1.10 ± 0.5	9.41
Cu(I) Pae	4.89 ± 0.5	3.98 ± 0.9	9.7 ± 2	9.9 ± 2	2.03 ± 0.9	15.2
Ni(II) Pae	11.5 ± 1	9.4 ± 2	22.9 ± 4	23.3 ± 4	4.8 ± 2	9.42
Co(II) Pae	26.1 ± 3	12.9 ± 3	31.5 ± 6	32.0 ± 6	6.6 ± 3	11.6
Hg(II) Pae	3.04 ± 0.3	2.47 ± 0.5	6.1 ± 1	6.2 ± 1	1.26 ± 0.5	2.43
Ag(I) Pae	0.0007 ± 0.0001	0.0006	0.001	0.001	0.0003	0.109
Cu(II) Afe	3.09 ± 0.03	4.54 ± 0.9	1.5 ± 1	1.0 ± 1	1.60 ± 0.8	4.23
Cu(I) Afe	1.77 ± 0.2	2.60 ± 0.6	0.89 ± 0.1	0.59 ± 0.6	0.92 ± 0.5	6.33
Hg(II) Afe	0.847 ± 0.09	1.24 ± 0.3	0.43 ± 0.3	0.28 ± 0.3	0.44 ± 0.2	0.839

[a] In the calculations of electronic energy transfer rates for metal ion derivatives of azurin Pae and Afe, the direction of the transition dipole moment in W48 and W118 is taken to be +70° and −20°, respectively, to the long axis of the indole ring. The column labeled J_{AD} lists values of overlap integrals calculated for each metalloazurin. The column labeled M–His lists energy transfer rates assuming the absorption transition moment is along one of the histidine to metal bonds and that both histidine to metal transitions are equal contributors to the absorption in the overlap region. The column labeled M–P_y lists expected energy transfer rates if the absorption transition moment lies along the line connecting the P_y orbital of the thiolate sulfur to the metal cation. The columns labeled M–Cys and M–Met list expected energy transfer rates if the absorption transition moment was along either the metal to cysteine or the metal to methionine bond, respectively. The column labeled observed rate is the metal-induced nonradiative rate defined in Table I.

azurin Pae may be slightly underestimated. This should not lead to a serious error in the calculated rates.

Energy transfer rates in azurin Pae and Afe were calculated with the data in Tables II–IV. It is assumed in these calculations that an overlap integral is associated exclusively with only one absorption transition dipole, except for metal–histidine transitions, where both His46 and His117 are assumed to have equal contributions.

Comparing the observed quenching rates to the calculated rates of energy transfer listed in Table IV, it is striking that an assignment of the acceptor to the metal-to-histidine transitions yields remarkable agreement with the experimental values for Ni(II), Co(II), and Hg(II) Pae and Cu(II) and Hg(II) azurin Afe. For Cu(II) and Cu(I) azurin Pae the observed rates are too fast for this assignment. For Cu(II) and Cu(I) azurin Pae, if the acceptor were the thiolate P_y orbital (see below), then the calculated times do match experiment. But this transition in Cu(II) azurins is assigned to an absorption at much lower wavelengths and is expected to be at much higher energies for Cu(I), since Cu(I) is more difficult to reduce than Cu(II). For Cu(I) azurin Afe and Ag(I) azurin Pae, all calculated rates are much too slow to match experiment.

Assignments of the various absorption bands of these and related metalloproteins have been discussed extensively by other workers. Ni(II) azurin Pae has a major absorption in the spectral overlap region at 355 nm. This has been assigned to a methionine LMCT (Tennent & McMillin, 1979) or to a histidine LMCT (Lum & Gray, 1981). Our results favor the latter histidine assignment, but the methionine assignment is not in major disagreement with experiment. Throughout this analysis, we have considered that only a single acceptor transition is responsible, though for the broad overlap found with azurin Afe other transitions could contribute. Nevertheless, with this assumption, a transition has been identified that leads to a calculated rate close to the observed rate, and inclusion of contributions from other transitions would reduce the calculated rate and cause a greater difference between calculated and experimental rates. For Co(II) azurin Pae the 333-nm absorption peak has been assigned to a thiolate LMCT (Tennent & McMillin, 1979) or to a thioether LMCT (Whelan & Bosnich, 1986). However, imidazole complexes of the Co(II) cation exhibit LMCT in the ultraviolet overlap region (Schugar, 1983). Again, the measured rate seems to favor the histidine assignment. The Hg(II) azurin Pae difference spectrum shows an absorption band ($\epsilon_{max} = 1.3 \times 10^3$ M cm^{-1} at 280 nm) extending into the overlap region. In Hg(II) plastocyanin this band was assigned to the thiolate LMCT transition (Tamilarasan & McMillin, 1986). For azurins Pae and Afe this assignment produces energy transfer rates either too rapid or too slow, respectively (Table IV). An assignment of this absorption to a Hg(II) metal to histidine ligand charge-transfer (MLCT) transition would be consistent with our experiments for both proteins.

In the case of Cu(II) azurin Pae a histidine assignment is not able to produce a rate that is sufficiently fast to explain the observed rate, and there seems no reason to assume that the uncertainty in the calculated rate is greater than for other systems. Although assigning the overlap region to a thiolate transition in Cu(II) azurins could explain the quenching of W48 in Cu(II) azurin Pae as energy transfer, such an assignment will not explain the quenching of W118 in Cu(II) azurin Afe. Fluorescence quenching of W118 from energy transfer requires assigning this region primarily to a histidine transition. Such an assignment is supported by studies using imidazole and pyrazole complexes of Cu(II) as model systems (Schugar, 1983; Bernarducci et al., 1981; Fawcett et al., 1980). Three LMCT transitions were shown to exist for tetragonal imidazole complexes of Cu(II) that have absorptions centered at 230, 260, and 330 nm (Fawcett, 1980). These transitions are expected to red shift 8000–12 000 cm^{-1} when the ligands are forced into a pseudotetrahedral geometry (Bernarducci, 1981) appropriate for azurin Cu(II) ligation. The red shifting of the two highest energy LMCT transitions would correspond to the broad absorption in the overlap region of Cu(II) azurins. The broadness of this weak feature can be explained in part by the nonequivalence of the two histidines (Solomon et al., 1986) and a possible methionine LMCT (Prochaska et al., 1981) absorption at longer wavelengths which contributes little to the overlap integral.

We have not measured a difference spectrum for Zn(II) azurin Pae. However, the difference spectrum for Zn(II) plastocyanin (Tamilarasan & McMillin, 1986) shows no absorption in the overlap region. Also, the reduction potential of Zn(II) in azurin is expected to be too high to allow electron transfer from an excited-state tryptophan residue. As expected, there is no significant quenching of the steady-state fluorescence (Engeseth, 1983), nor is there a fast component to the fluorescence decay. Thus for most of the metalloazurins the dominant quenching mechanism seems to be electronic energy transfer, and there is no compelling reason to invoke a long-range electron transfer process.

(*2*) *Reductive Fluorescence Quenching.* Ag(I) azurin Pae has a very small overalp integral (see Figure 5), and even the modest observed quenching does not seem to be explainable with electronic energy transfer. Nor is an enhanced intersystem crossing from a heavy-atom influence from silver a quenching mechanism, since the fluorescence to phosphorescence ratio of Ag(I) azurin Pfl is similar to that of apozurin Pfl (Finazzi Agro et al., 1973). Ag(II) can be stable in certain ligand environments (Barefield & Mocella, 1973), so it is possible that reductive quenching accounts for the rate of fluorescence decay in Ag(I) azurin Pae, i.e.

$$Trp^* \; Ag(I) \rightarrow Trp^{\bullet +} \; Ag(II)$$

The origin of the absorption in the Cu(I) azurin difference spectrum with a maximum at 280 nm is not certain. An analogous absorption in the difference spectrum of plastocyanin has been assigned to one of three possibilities (Tamilarasan & McMillin, 1986): a charge transfer to solvent, a Rydberg transition, or a MLCT to the histidines. A charge-transfer to solvent transition seems unlikely, since the metal center in azurin Pae is buried in the protein and not accessible to solvent (Mallinson et al., 1981; Chothia & Lesk, 1982). The most likely assignment for this absorption is a MLCT to the histidines. Assigning this absorption to a cysteine transition gives a rate of energy transfer that agrees with experiment for Cu(I) azurin Pae, but not for Cu(I) azurin Afe. All other ligand–metal transitions provide calculated rates of energy transfer that are much too slow. It would seem that electronic energy transfer is not the major quenching mechanism. A possible quenching mechanism is a reductive quenching. The intersystem crossing rate is increased as mentioned earlier, since Cu(I) azurin Pfl has a triplet-state quantum yield for tryptophan that is higher than for other metal derivatives of azurin Pfl. This observation indicates an interaction between Cu(I) and excited singlet of W48 in azurin Pfl.

(*3*) *Oxidative Fluorescence Quenching.* The significantly larger discrepancy between calculated and measured quenching rates for Cu(II) azurin Pae raises the possibility of a different mechanism for fluorescence quenching. Turoverov et al.

(1985) have remarked that the spectral overlap between azurin Pfl fluorescence and its ultraviolet absorption was insufficient to explain the observed fluorescence quenching, though no quantitative analysis was provided in their report. We have previously suggested that the quenching in Cu(II) azurins results from an oxidative quenching of the tryptophan, i.e.

$$Trp^* Cu(II) \rightarrow Trp^{\bullet+} Cu(I)$$

An estimation of the free energy change for this reaction implies an activationless electron transfer. If we add to the reorganization energy of the tryptophan [see Petrich et al., (1987)] 0.3 eV for the reorganization energy of the ligands surrounding the copper (Margalit et al., 1984), then the total reorganization energy of 1.05 eV is almost identical with the free energy change ($-\Delta G^\circ$ = 1.07 eV; Petrich et al., 1987). Thus, electron transfer could proceed at the maximum Marcus rate and will be activationless. As Table I shows, the fast component in Cu(II) azurin Pae depends very weakly on temperature. Of course such a behavior is also expected for an energy transfer process, since the fluorescence of azurin Pae shifts little with temperature. The possibility that electron transfer is important in Cu(II) azurin Pae cannot be ruled out. However, given the success of energy transfer calculations with other metalloazurins, it seems most likely that energy transfer is the quenching mechanism here too. We do not understand why the calculated rate differs from the experimental value by a larger factor than found for other metalloazurins. However, even in this case the maximum discrepancy is a factor of 4.

If electron transfer were responsible for the quenching of the solvent-exposed W118 of azurin Afe, one would expect a much greater reduction in rate than the observed factor of 2 (Table I) because of the greatly increased reorganization energy. Studies on long-range electron transfer in ruthenium-modified proteins (Mead et al., 1989) suggest that when either donor or acceptor is exposed to an aqueous environment, the rate is reduced by 6 orders of magnitude. Similar arguments apply to the Cu(I) azurins Pae and Afe, if reductive quenching is involved in both cases. The remarkable consistency of the ratios of $k_{MI}(Pae)/k_{MI}(Afe)$ for Cu(II), Cu(I), and Hg(II) azurins could be taken as a hint of a common mechanism.

As previously mentioned, we attribute the long lifetime component to an apo-like impurity which is unable to bind metal cations. Schimmel (1989) has pointed out the possibility of small amounts of a mistranslational protein being a possible cause of contaminating proteins which are inactive. Hutnik and Szabo (1989a) have explained their multicomponent fits to be the result of conformational heterogeneity, yet they do not give a mechanism for how this would lead to very different fluorescence quenching rates. In particular, they attribute the long component to a conformation wherein the metal–ligand complex is situated far away from the tryptophan residue. If the quenching mechanism is either electron transfer or electronic energy transfer, it seems unlikely that a change in conformation could create a large enough change in distance or orientation to turn off the quenching, while still maintaining the unique blue fluorescence spectrum of azurin Pae that is a consequence of a hydrophobic environment.

Conclusions

Fluorescence quenching of the metal derivatives of azurin can be explained by an electronic energy transfer. With restricted orientations for the dipole moments of donor and acceptor, Forster calculation of energy transfer rates are within 20% of observed fluorescence decay rates, in most cases. With Cu(II) azurin Pae a significantly larger discrepancy is obtained, and while energy transfer quenching remains the likely mechanism, the possibility of electron transfer cannot be ruled out. Comparison of the calculated rate of energy transfer to the observed rate of quenching in Cu(II) azurin Afe supports the view that the absorption in the overlap region is predominantly from histidine LMCT transitions. It should be pointed out that although the overlap integral for Cu(II) azurin Pae is small, it is not insignificant, as once thought (Turoverov et al., 1985). Calculated rates of energy transfer for both Hg(II) azurin Pae and Hg(II) azurin Afe are consistent with experiment if the absorption in the overlap region is assigned to a metal to histidine MLCT. The fluorescence quenching of Co(II) and Ni(II) azurin Pae can also be explained by energy transfer. The calculated rates of energy transfer for metalloazurins Afe were based on orientations for the tryptophan W118 obtained from a molecular dynamics simulation of Chen et al. (1988) and lends experimental support to their calculation.

Fluorescence quenching as a result of electron transfer may play a major role in Ag(I) azurin Pae, and possibly in Cu(II) and Cu(I) azurin Pae and in Cu(I) azurin Afe. The only quenching mechanism available to Ag(I) azurin Pae is reductive quenching. Although reductive quenching may also be possible for Cu(I) azurins, a much greater decrease in the observed rate for the Afe than a factor of 2 compared to the rate of Pae is expected (due to the greater reorganization energy for the solvent around W118).

The difference absorption spectra of the metal derivatives of azurin Pae are very similar to those of the analogous metal derivatives of plastocyanin (Tamilarasan & McMillin, 1986). This further demonstrates the similarities of the metal binding sites among the blue copper proteins. The tryptophan difference that appears in the metalloazurin difference spectrum may be correlated with the charge on the metal. Cu(II) blue shifts the absorption, while Cu(I) and Ag(I) red shift the absorption. Further, the relative intensity of the tryptophan difference in the Cu(I) azurin Pae difference spectrum is considerably larger than those of the other metal derivatives. This suggests that the tryptophan in azurin Pae is perturbed more by Cu(I) than the other metal cations with respect to tryptophan in apoprotein.

Acknowledgments

We thank Professor Russell Timkovich (University of Alabama) for making available to us purified azurin Pae and Afe. We thank Dr. Vicky Hines for her assistance with purification and preparation of the proteins. We are grateful to Professor Michael Johnston (University of Chicago) for use of his laboratory facilities to purify the azurins and to make the metal derivatives. Molecular graphics were provided to us by Professor James Norris (University of Chicago). We appreciate detailed discussions with Professor David McMillin (Purdue University) on the spectroscopy of azurins.

References

Adman, E. T., & Jensen, L. H. (1981) *Isr. J. Chem. 21*, 8–12.

Ainscough, E. W.; Bingham, A. G., Brodie, A. M., Ellis, W. R., Gray, H. B., Loehr, T. M., Plowman, J. E., Norris, G. E., & Baker, E. N. (1987) *Biochemistry 26*, 71–82.

Ambler, R. P. (1973) in *Recent Developments in Chemical Studies of Protein Structures* (Previero, A., Pechere, J. F., & Coletti-Previero, M. A., Eds.) pp 289–305, INSERM, Paris.

Ambler, R. P., & Brown, L. H. (1967) *Biochem. J. 104*, 784–825.

Ambler, R. P., & Tobari, J. (1989) *Biochem. J. 261*, 495–499.

Baker, E. N. (1988) *J. Mol. Biol. 203*, 1071–1095.
Barefield, K. E., & Mocella, M. T. (1973) *Inorg. Chem. 12*, 2829–2832.
Bashford, D., Karplus, M., & Canters, G. W. (1988) *J. Mol. Biol. 203*, 507–510.
Bernarducci, E., Schwindinger, W. F., Hughey, J. L., Krogh-Jespersen, K., & Schugar, H. J. (1981) *J. Am. Chem. Soc. 103*, 1686–1691.
Blaszak, J. A., McMillin, D. R., Thornton, A. T., & Tennent, D. L. (1983) *J. Biol. Chem. 258*, 9886–9892.
Chen, L. X.-Q., Engh, R. A., Brunger, A. T., Nguyen, D. T., Karplus, M., & Fleming, G. R. (1988) *Biochemistry 27*, 6908–6921.
Chothia, C., & Lesk, A. M. (1982) *J. Mol. Biol. 160*, 309–323.
Church, W. B., Guss, J. M., Potter, J. J., & Freeman, H. C. (1986) *J. Mol. Biol. 261*, 234–237.
Colman, P. M., Freeman, H. C., Guss, J. M., Murata, M. Norris, V. A., Ramshaw, J. A. M., & Venkatappa, M. P. (1978) *Nature 272*, 319–324.
Donovan, J. W. (1969) in *Physical Principles and Techniques of Protein Chemistry* (Leach, S. J., Ed.) Part A, pp 101–120, Academic Press, New York.
Engeseth, H. R. (1983) Ph.D. Thesis, Purdue University.
Engeseth, H. R., & McMillin, D. R. (1986) *Biochemistry 25*, 2448–2455.
Engeseth, H. R., McMillin, D. R., & Otvos, J. D. (1984) *J. Biol. Chem. 259*, 4822–4826.
Fawcett, T. G., Bernarducci, E. E., Krogh-Jespersen, K., & Schugar, H. J. (1980) *J. Am. Chem. Soc. 102*, 2598–2604.
Finazzi-Agro, A., Giovagnoli, C., Avigliano, L., Rotilio, G., & Mondovi, B. (1973) *Eur. J. Biochem. 34*, 20–24.
Forster, T. (1948) *Ann. Phys. (Leipzig) 2*, 55–57.
Forster, T. (1959) *Discuss. Faraday Soc. 27*, 7–17.
Forster, T. (1965) in *Modern Quantum Chemistry* (Sinanoglu, O., Ed.) Part III, pp 93–137, Academic, New York.
Garret, T. P. J., Clingeleffer, D. J., Guss, J. M., Rodgers, S. J.s, & Freeman, H. C. (1984) *J. Biol. Chem. 259*, 2822–2825.
Grinvald, A., Schlessinger, J., Pecht, I., & Steinberg, I. Z. (1975) *Biochemistry 14*, 1921–1929.
Hansen, J. E., Longworth, J. W., & Fleming, G. R. (1988) *Photochem. Photobiol. 47* (Suppl.), 12S.
Hauenstein, B. L., Jr., & McMillin, D. R. (1981) *Met. Ions Biol. Syst. 13*, 319–347.
Henry, Y., & Bessiere, P. (1984) *Biochimie 66*, 259–289.
Hochstrasser, R. M., & Negus, D. K. (1984) in *Proteins of Biological Structure and Dynamics* (Szabo, A. G., & Masotti, L., Eds.) p 165, Plenum Press, London.
Hutnik, C. M., & Szabo, A. G. (1989a) *Biochemistry 28*, 3923–3934.
Hutnik, C. M., & Szabo, A. G. (1989b) *Biochemistry 28*, 3935–3939.
Korszum, Z. R. (1987) *J. Mol. Biol. 196*, 413–415.
Lami, H., & Glasser, N. (1986) *J. Chem. Phys. 84*, 597–604.
Lever, A. B. P. (1984) in *Inorganic Electronic Spectroscopy*, 2nd ed., pp 679–734, Elsevier, New York.
Live, D. H., Kojiro, C. L., Cowburn, D., & Markley, J. L. (1985) *J. Am. Chem. Soc. 107*, 3043–3045.
Lum, V., & Gray, H. B. (1981) *Isr. J. Chem. 21*, 23–25.
Mallinson, R., Carter, R., & Ghiron, C. A. (1981) *Biochim. Biophys. Acta 671*, 117–122.
Margalit, R., Kostic, N. M., Che, C.-M., Blair, D. F., Chiang, H.-J., Pecht, I., Shelton, J. B., Shelton, J. R., Schroeder, W. A., & Gray, H. B. (1984) *Proc. Natl. Acad. Sci. U.S.A. 81*, 6554–6558.
Marcus, R. A., & Sutin, N. (1985) *Biochim. Biophys. Acta 811*, 265–322.
McMillin, D. R., Holwerda, R. A., & Gray, H. B. (1974) *Proc. Natl. Acad. Sci. U.S.A. 71*, 1339–1341.
Mead, T. J., Gray, H. B., & Winkler, J. R. (1989) *J. Am. Chem. Soc. 111*, 4353–4356.
Negus, D. K. (1985) Ph.D. Thesis, University of Pennsylvania.
Norris, G. E., Anderson, B. F., & Baker, E. N. (1983) *J. Mol. Biol. 165*, 501–521.
Norris, G. E., Anderson, B. F., & Baker, E. N. (1986) *J. Am. Chem. Soc. 108*, 2784–2785.
Pecht, I., Farver, O., & Goldberg, M. (1977) *Adv. Chem. Ser. 162*, 179–206.
Penfield, K. W., Gewirth, A. A., & Solomon, E. I. (1985) *J. Am. Chem. Soc. 107*, 4519–4529.
Petrich, J. W., Longworth, J. W., & Fleming, G. R. (1987) *Biochemistry 26*, 2711–2722.
Philips, P. A., & Levy, D. H. (1986) *J. Chem. Phys. 85*, 1327–1332.
Prochaska, H. J., Schwindinger, W. F., Schwartz, M., Burk, M. J., Bernarducci, E., Lalancette, R. A., Potenza, J. A., & Schugar, H. J. (1981) *J. Am. Chem. Soc. 103*, 3446–3455.
Rehms, A. A., & Callis, P. R. (1987) *Chem. Phys. Lett. 140*, 83–89.
Richardson, J. (1982) *Adv. Protein Chem. 34*, 167–339.
Ruggiero, A. J., Todd, D. C., & Fleming, G. R. (1990) *J. Am. Chem. Soc. 112*, 1003–1014.
Ryden, L. (1984) in *Copper Proteins and Copper Enzymes* (Lontie, R., Ed.) Vol. 1, pp 157–182, CRC Press, Boca Raton, FL.
Schimmel, P. (1989) *Acc. Chem. Res. 22*, 232–233.
Schugar, H. J. (1983) in *Copper Coordination Chemistry: Biochemical and Inorganic Perspectives* (Karlin, K. D., & Zubieta, J., Eds.) pp 43–74, Adenine Press, Guilderland, N.Y.
Solomon, E. I., Gerwirth, A. A., & Cohen, S. L. (1986) in *Excited States and Reactive Intermediates* (Lever, A. B. P., Ed.) ACS Symposium Series 307, pp 236–266, American Chemical Society, Washington, DC.
Strickland, E. H. (1974) *CRC Crit. Rev. Biochem. 2*, 114–175.
Szabo, A. G., Stepanik, T. M., Wayner, D. M., & Young, N. M. (1983) *Biophys. J. 41*, 233–244.
Tamilarasan, R., & McMillin, D. R. (1986) *Inorg. Chem. 25*, 2037–2040.
Tennent, D. L., & McMillin, D. R. (1979) *J. Am. Chem. Soc. 101*, 2307–2311.
Turoverov, K. K., Kuznetsova, I. M., & Zaitsev, V. N. (1985) *Biophys. Chem. 23*, 79–89.
Ugurbil, K., Maki, A. H., & Bersohn, R. (1977) *Biochemistry 16*, 901–907.
Whelan, J., & Bosnich, B. (1986) *J. Am. Chem. Soc. 25*, 3671–3675.
Yamamoto, Y., & Tanaka, J. (1972) *Bull. Chem. Soc. Jpn. 45*, 1362–1366.